Heliyon 10 (2024) e33092

Contents lists available at ScienceDirect

Heliyon

journal homepage: www.cell.com/heliyon

Research article

Identification of disulfidptosis-related clusters and construction of a disulfidptosis-related gene prognostic signature in triple-negative breast cancer

Jie Wu [a,*], Yan Cai [b], Gaiping Zhao [c]

[a] Key Laboratory of Hydrodynamics (Ministry of Education), School of Ocean and Civil Engineering, Shanghai Jiao Tong University, Shanghai, 200240, China
[b] School of Biological Science and Medical Engineering, Southeast University, Nanjing, 210096, China
[c] School of MedicalInstrumentandFoodEngineering, University ofShanghai forScience and Technology, Shanghai, 200093, China

ARTICLE INFO

Keywords:
Disulfidptosis
Gene prognostic signature
Nomogram
Immunotherapy

ABSTRACT

Objective: This study aimed to explore disulfidptosis-related clusters of triple-negative breast cancer (TNBC) and build a reliable disulfidptosis-related gene signature for forecasting TNBC prognosis.
Methods: The disulfidptosis-related clusters of TNBC were identified based on public datasets, and a comparative analysis was conducted to assess their differences in the overall survival (OS) and immune cell infiltration. Morever, the differentially expressed genes (DEGs) between clusters were recognized. Then, the prognostic DEGs were then chosen. A prognostic signature was constructed by the prognostic DEGs, followed by nomogram construction, drug sensitivity, immune correlation, immunotherapy response prediction, and cluster association analyses.
Results: Two disulfidptosis-related clusters of TNBC were identified, which had different OS and macrophage infiltration. Moreover, 235 DEGs were identified between two clusters. A prognostic signature was then constructed by five prognostic DEGs including HLA-DQA2, CCL13, GBP1, LAMP3, and SLC7A11. This signature was highly valuable in predicting prognosis. A nomogram was built by risk score and AJCC stage, which could forecast OS accurately. Moreover, patients with high-risk scores exhibited greater sensitivity to chemotherapy drugs such as lapatinib and had a lower immunotherapy response.
Conclusions: Two TNBC clusters linked to disulfidptosis were identified, with different OS and immune cell infiltration. Moreover, a five-disulfidptosis-related gene signature may be a powerful prognostic biomarker for TNBC.

1. Introduction

Triple-negative breast cancer (TNBC) is recognized for its aggressive nature and makes up around 15–20 % of the total breast cancer diagnoses [1]. It is a heterogeneous disease that is defined by the negative expression of progesterone receptor, estrogen receptor, and human epidermal growth factor receptor 2 [2]. In the first five years after diagnosis, the mortality rate of TNBC in the advanced stage is

* Corresponding author. School of Ocean and Civil Engineering, Shanghai Jiao Tong University, No.800 Dongchuan Road, Minhang District, Shanghai, 200240, China.
E-mail address: jiewu82@sjtu.edu.cn (J. Wu).

https://doi.org/10.1016/j.heliyon.2024.e33092
Received 13 December 2023; Received in revised form 4 June 2024; Accepted 13 June 2024
Available online 14 June 2024

as high as 40 % [3]. As there are no receptors that can be effectively targeted, the systemic treatment of TNBC still relies on chemotherapy, however, over 50 % TNBC patients experience recurrence after chemotherapy [4,5]. Recently, the incorporation of targeted therapies, immunotherapy, and novel treatment strategies has revolutionized the management of breast cancer, offering improved outcomes and personalized approaches for patients [6–9]. This shift underscores the critical need to delve deeper into the key mechanism affecting TNBC prognosis. Understanding these underlying processes is essential for developing more precise therapeutic targets and improving prognostic assessments, ultimately leading to more effective and tailored treatment options for TNBC patients.

Disulfide metabolism describes the cellular redox control exerted by the dynamic balance of disulfide bond fformation and breakdown. A growing body of research indicates that disulfide metabolism is intricately linked to the biological behaviors of cancer cells, like metastasis, immune evasion, and resistance to drugs [10,11]. Recently, disulfidptosis represents a novel form of regulated cell death caused by the stress induced by high levels of cystine inside the cell, which pertains to disulfide metabolism [12]. Glucose-deprived cancer cells with elevated SLC7A11 expression accumulate excessive disulfide substances, which interrupts the disulfide bond connections between cytoskeletal proteins, causing the disintegration of the histone framework and ultimately cell death, a process termed disulfidptosis. In addition, disulfidptosis plays a significant role in cancer metabolic therapy [13]. A very recent study shows that the disulfidptosis suppressor genes, such as SLC3A2, RPN1, SLC7A11, and NCKAP1, are implicated in bladder cancer pathogenesis [14]. However, the exact involvement of disulfidptosis in TNBC remains largely unclear. Exploration of disulfidptosis-related tumor subtypes and genes will help to predict disease risk and improve prognosis of TNBC.

Here, we retrieved publicly available gene expression and clinical data for TNBC samples and obtained genes linked to disulfidptosis from a publication by Lin et al. [12]. We then identifed disulfidptosis-related clusters and compared their differences in overall survival (OS), clinical feature distribution, immune cell infiltration, and enriched hallmark gene sets. Morever, we analyzed the differentially expressed genes (DEGs) between clusters and selected prognostic DEGs. A disulfidptosis-related prognostic signature was then bulit, followed by nomogram construction, drug sensitivity analysis, immune correlation analysis, immunotherapy response prediction, and cluster association analysis. We hope to reveal the key molecular mechanisms related to disulfidptosis in TNBC development, and explore promising biomakers for predicting TNBC prognosis.

2. Data and methods

2.1. Data acquisition and preprocessing

The breast cancer-related gene expression and clinical data were obtained from TCGA database. The gene expression profile was re-annotated, and the mRNA expression profile was extracted. The TNBC samples that were ER, PR and HER-2 negative were extracted through clinical data. The samples without survival time were then removed. Finally, 120 TNBC samples with prognostic information and 113 normal samples were retained for subsequent analysis.

Meanwhile, GSE103091 and GSE103668 datasets were downloaded from NCBI GEO database. Following the exclusion of samples lacking survival time, 107 TNBC samples in GSE103091 were retained for validation of the prognostic signature. GSE103668 dataset included 21 TNBC samples treated with cisplatin and bevacizumab in the neoadjuvant setting, which was used for validating immunotherapy response of different risk groups.

2.2. Acquiring of disulfidptosis-related genes

According to the information published by Lin et al. [12], ten disulfidptosis-related genes were acquired. Based on TCGA-TNBC data, their expression differences between TNBC and normal sample were analyzed. Then, the mutation frequency of these genes was analyzed using R maftools package (version 2.8.0) [15], and the gene mapping was drawn using RCircos package (version 1.2.2) [16].

2.3. Identification of disulfidptosis-related clusters

Based on the gene expression matrix of disulfidptosis-related genes, tumor cluster analysis on the TCGA-TNBC samples was employed using R ConsensusClusterPlus package (version 1.54.0) [17]. The optimal TNBC clusters (K value) were analyzed. Then, gene set variation analysis (GSVA) was performed to evaluate the disulfidptosis score of each TNBC sample utilizing R GSVA package (version 1.36.3) [18]. The difference in the disulfidptosis score between different clusters was compared using Wilcoxon test.

2.4. Cluster survival and clinical feature correlation analysis

To compare the OS differences between clusters, Kaplan–Meier (K–M) curves were conducted using R survival (version 2.41-1) package [19]. By integrating clinical information data of TNBC, the distribution of clinical features (age, TNM staging, tumor stage, and PAM50Call) between different clusters was compared using Chi-square test.

2.5. Immune infiltration analysis for different clusters

To observe immune microenvironment difference of different clusters, the infiltration of immune cell types in tumor samples was

analyzed using CIBERSORT [20] and ssGSEA [21] algorithms. Then, the ESTIMATE, immune, and stromal scores were calculated using R ESTIMATE package [22]. Moreover, the gene expression data of immune checkpoint-related genes and human leukocyte antigen (HLA) family genes were extracted based on TCGA-TNBC dataset. Comparative analysis of immune indices and gene expression between different clusters were performed through Wilcoxon test.

2.6. GSEA

The differentially enriched hallmark gene sets between different clusters were analyzed using GSEA algorithm [23]. The cutoff value was $P < 0.05$ and $|\text{normalized enrichment score}| > 1$.

2.7. DEGs identification

Based on TCGA-TNBC data, the DEGs between different clusters were recognized using limma package (version 3.34.7) [24]. DEGs were selected with $|\text{fold change}| \geq 2$ and Benjamini-Hochberg-adjusted P value < 0.05.

2.8. Construction of the prognostic signature

By combining the gene expression with the OS information of each patient, univariate Cox regression analysis was employedto screen prognostic genes with $P < 0.05$. A prognostic signature was established via stepwise Cox regression analysis using R survminer package (version 0.4.9) [25]. The risk score was calculated as follows: risk score $= h(t, X) = h_0(t) * \exp(\beta_1X_1 + \beta_2X_2 + \ldots + \beta_nX_n)$, where β represents the regression coefficient, ho (t) is the benchmark risk rate; and h (t, X) indicates the risk rate associated with X (covariable) at time t.

The risk score of each patient in the TCGA training dataset and GSE103091 dataset was calculated. According the median risk score, patients from both datasets were stratified into high- or low-risk groups. K–M curves analysis was employed to evaluate the disparities inOS between the two risk groups.

2.9. Analysis of the prognostic independence of risk score

To investigate the independence of risk score in predicting prognosis, the clinical factors of TNBC patients and risk score were included into univariate and multivariate Cox regression analyses. Prognostic factors with independent value were identified with $P < 0.05$.

2.10. Establishment of a nomogram

Using the independent prognostic factors, we developed a nomogram using R rms package (version 5.1-2) [26] to evaluate the OS probabilities of TNBC patients. Calibration curves were plotted to assess the validity of the nomogram. According to the median value of nomogram score, the TNBC patients were classified into high- or low-score groups and their OS differences were analyzed using Kaplan–Meier curves. Meanwhile, the performance of this nomogram in predicting OS probabilities was assessed by receiver operating characteristic (ROC) curves that was plotted using timeROC (version 0.4) [27].

2.11. Drug sensitivity analysis for two risk groups

The sensitivity of chemotherapy drugs in each patient was evaluated based on the CDSC database. The IC50 value of drugs was quantified using R pRRophetic package [28]. The difference in IC50 value of each chemotherapy drug between two risk groups was quantified using the Wilcoxon test.

2.12. Association analysis of risk score with immunity

The proportion of 24 kinds of immune cells in TCGA-TNBC samples was analyzed using ssGSEA algorithm. Then, the link between signature genes and immune cell infiltration level was examined.

2.13. Immunotherapy response prediction

The immunotherapy response of each patient was evaluated using the TIDE database. The cytolytic activity (CYT) scores were defined as mean values of GZMA and PRF1 expression. Tertiary lymphoid structure (TLS) score was calculated by GSVA algorithm for TLS characteristic genes (CCR6, CETP, CD79B, CD1D, PTGDS, RBP5, LAT, EIF1AY, and SKAP1). Through Wilcoxon test, the TIDE scores, CYT scores, and TLS scores between two risk groups were compared. Additionally, the GSE103668 dataset was utilized to analyze the risk score difference between treatment response and non-response groups.

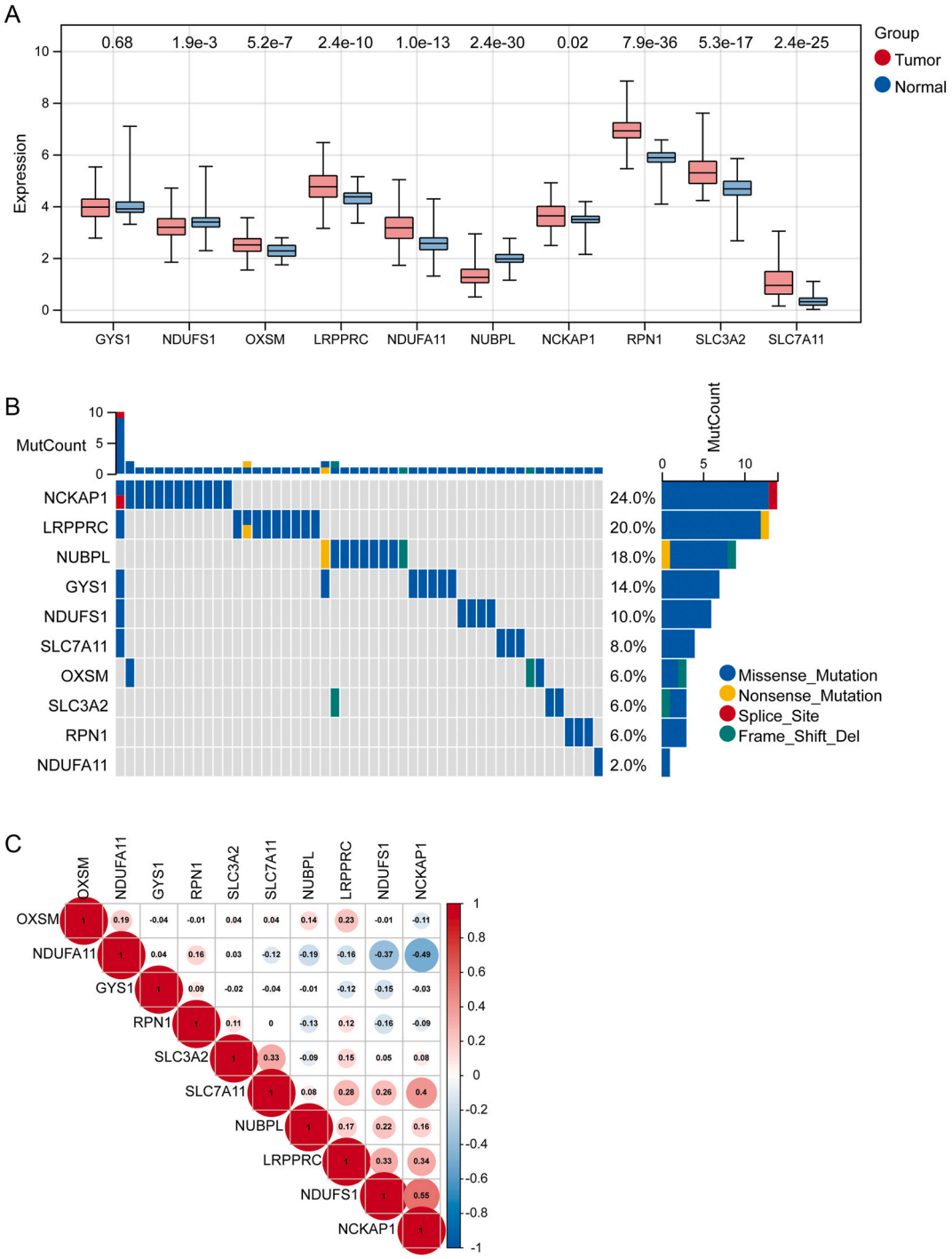

Fig. 1. Analysis of disulfidptosis-related genes based on TCGA-TNBC data. A: The expression difference of 10 disulfidptosis-related genes between tumor and normal samples. B: The mutation frequency of disulfidptosis-related genes. C: The correlation of Based on TCGA-TNBC data genes in tumor samples.

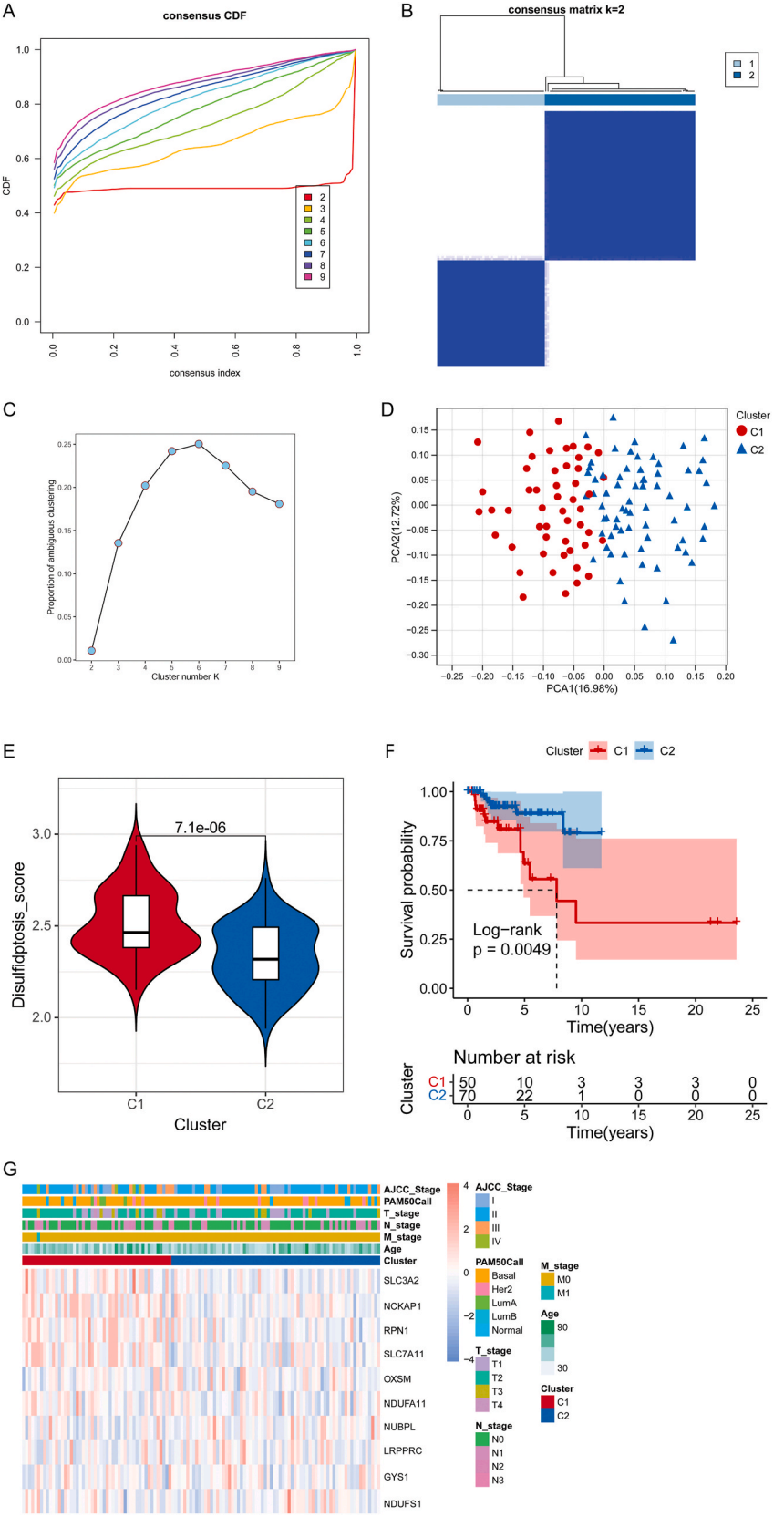

(caption on next page)

Fig. 2. Identification of disulfidptosis-related clusters. A: Cumulative distribution function (CDF) distribution curve. B: Heatmap of disulfidptosis-related clusters. C: Delta area line graph. D: Principal component analysis (PCA) plot of sample distribution in the two clusters. E: Comparison of disulfidptosis score of two clusters. F: Kaplan–Meier survival curve of two clusters. G: Heat maps of disulfidptosis-related gene expression in two clusters and their correlation with different clinical information. Red indicates high expression and blue indicates low expression. (For interpretation of the references to colour in this figure legend, the reader is referred to the Web version of this article.)

2.14. Association analysis between tumor clusters and different risk groups

According to the sample information, the association between different risk groups and tumor clusters was observed.

3. Results

3.1. Analysis of disulfidptosis-related genes

Based on TCGA-TNBC data, we analyzed the expression of ten disulfidptosis-related genes, including NDUFS1, NDUFA11, OXSM, GYS1, LRPPRC, SLC3A2, RPN1, NCKAP1, NUBPL, and SLC7A11. The results showed that except for GYS1, all other genes exhibited significant differential expression between tumor and normal group (Fig. 1A). In terms of mutation frequency, NCKAP1 had the highest incidence at 24 %, followed by LRPPRC at 20 %, and NUBPL at 18 %. Fig. 1B illustrated the mutation frequency of these genes. The correlation of these genes in tumor samples was shown in Fig. 1C.

3.2. Identification of disulfidptosis-related clusters

On basis of the expression data of disulfidptosis-related genes, TNBC samples were clustered into two clusters (Fig. 2A–C). PCA displayed that samples within the same cluster were clustered together (Fig. 2D). Moreover, the disulfidptosis score was found to be significantly greater in cluster 1 (C1) than in cluster 2 (C2) (Fig. 2E), confirming the scientific rationality of two clusters.

3.3. Survival and clinical feature correlation analysis for two clusters

The Kaplan-Meier curve analysis showed a significantly shorter OS time of C1 relative to C2, indicating that C1 had showed a worse prognosis than C2 (Fig. 2F). We collated clinical information of TNBC patients and found that only AJCC stage showed significant difference between two clusters ($p = 0.04$) (Table 1). The correlation heatmap of disulfidptosis-related genes with clinical characteristics of TNBC patients was shown in Fig. 2G.

Table 1
The clinical characteristics of TNBC samples in two disulfidptosis-related clusters.

Characteristics	C1(N = 50)	C2(N = 70)	Total (N = 120)	Pvalue
Age				0.66
>60	17 (14.17 %)	20 (16.67 %)	37 (30.83 %)	
≤60	33 (27.50 %)	50 (41.67 %)	83 (69.17 %)	
M_stage				0.87
M0	49 (40.83 %)	70 (58.33 %)	119 (99.17 %)	
M1	1 (0.83 %)	0 (0.0e+0 %)	1 (0.83 %)	
N_stage				0.14
N0	29 (24.17 %)	47 (39.17 %)	76 (63.33 %)	
N1	11 (9.17 %)	18 (15.00 %)	29 (24.17 %)	
N2	7 (5.83 %)	2 (1.67 %)	9 (7.50 %)	
N3	3 (2.50 %)	3 (2.50 %)	6 (5.00 %)	
T_stage				0.61
T1	13 (10.83 %)	14 (11.67 %)	27 (22.50 %)	
T2	30 (25.00 %)	50 (41.67 %)	80 (66.67 %)	
T3	6 (5.00 %)	5 (4.17 %)	11 (9.17 %)	
T4	1 (0.83 %)	1 (0.83 %)	2 (1.67 %)	
PAM50Call				0.14
Basal	40 (33.33 %)	58 (48.33 %)	98 (81.67 %)	
Her2	3 (2.50 %)	7 (5.83 %)	10 (8.33 %)	
LumA	4 (3.33 %)	0 (0.0e+0 %)	4 (3.33 %)	
LumB	0 (0.0e+0 %)	1 (0.83 %)	1 (0.83 %)	
Normal	3 (2.50 %)	4 (3.33 %)	7 (5.83 %)	
AJCC_Stage				0.04
I	8 (6.67 %)	12 (10.00 %)	20 (16.67 %)	
II	27 (22.50 %)	48 (40.00 %)	75 (62.50 %)	
III	11 (9.17 %)	10 (8.33 %)	21 (17.50 %)	
IV	4 (3.33 %)	0 (0.0e+0 %)	4 (3.33 %)	

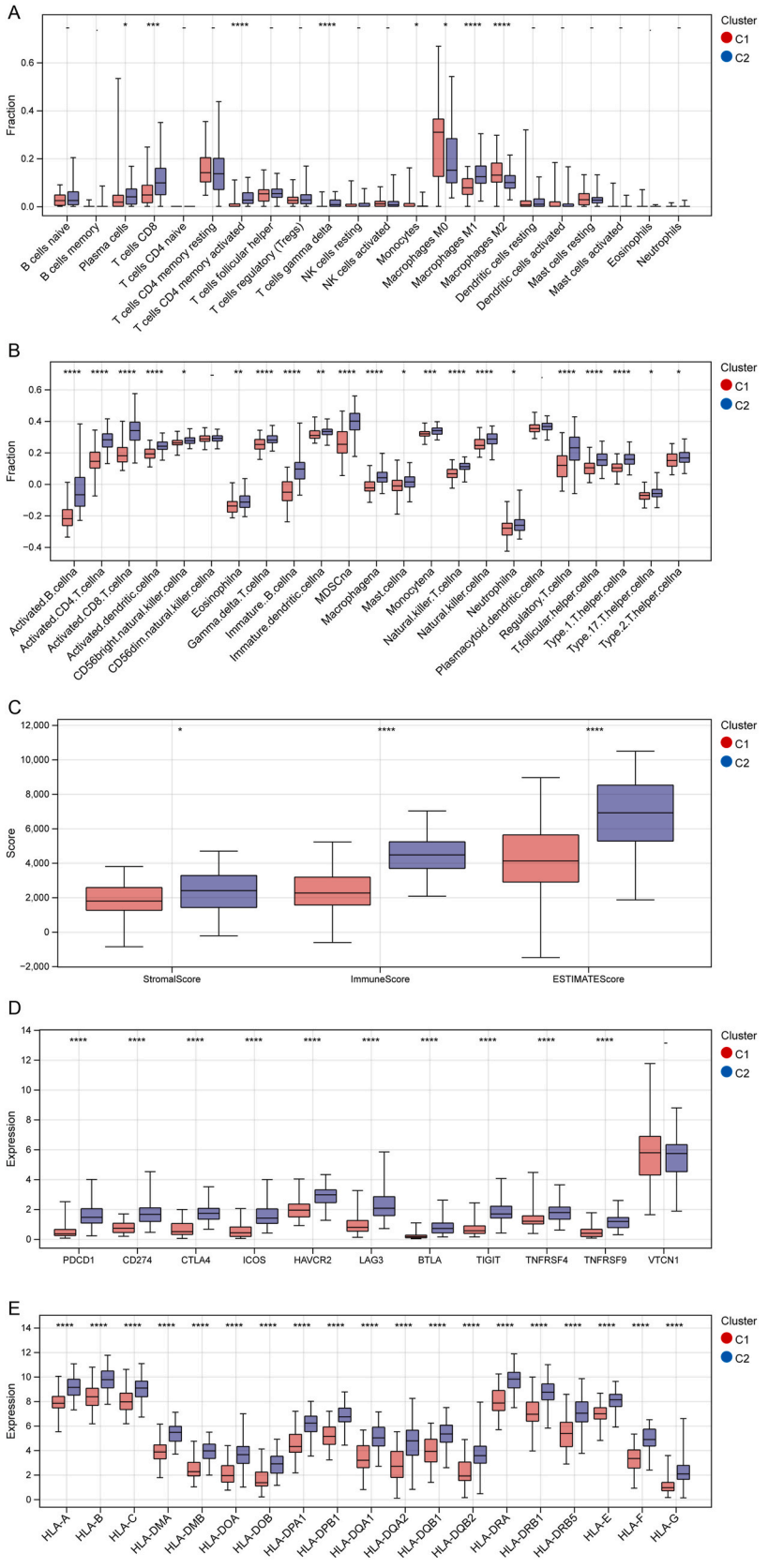

(caption on next page)

Fig. 3. Comparison of immune microenvironment between two clusters. A: The results of immune cell infiltration between two clusters using CIBERSORT algorithm. B. The results of immune cell infiltration between two clusters using the ssGSEA algorithm. C. The results of ESTIMATE score, immune score, and stromal score between two clusters using the ESTIMATE analysis. D. The expression of immune checkpoint genes between two clusters. E: The expression of HLA family genes between two clusters. *P < 0.05, **P < 0.01, ***P < 0.001, and ****P < 0.0001.

3.4. Immune infiltration analysis for two clusters

Utilizing TCGA-TNBC data, the CIBERSORT analysis demonstrated that eight types of immune cells were significantly different between two clusters, including T cells gamma delta, plasma cells, T cells CD4 memory activated, T cells CD8, macrophages M0, macrophages M1, monocytes, and macrophages M2 (Fig. 3A). The ssGSEA analysis revealed 22 differential immune cells between two clusters (Fig. 3B). Notably, both algorithms revealed that the infiltration proportion of macrophages had significant difference between two clusters. Moreover, C2 exhibited dramatically higher ESTIMATE, immune, and stromal scores than C1 (Fig. 3C). In addition, except for VTCN1, the other ten immune checkpoint genes including CTLA4, LAG3, ICOS, CD274, PDCD1, HAVCR2, TNFRSF9, BTLA, TNFRSF4, and TIGIT displayed a significant increase in expression in C2 compared to C1 (Fig. 3D). Furthermore, all the HLA family genes exhibited markedly increased expression in C2 (Fig. 3E).

3.5. GSEA

To observe the difference in biological function of two clusters, GSEA was conducted. The results displayed that there were 14 differentially enriched hallmark gene sets between two clusters, such as apoptosis, inflammatory response, and interferon gamma response (Fig. 4A).

3.6. Analysis of DEGs between two clusters and identification of prognostic genes

In total, 235 DEGs were identified between two clusters (Fig. 4B).

3.7. Validation of the prognostic signature

Using stepwise Cox regression analysis, five genes including HLA-DQA2, CCL13, GBP1, LAMP3, and SLC7A11 were selected for building prognostic signature (Fig. 5A). The risk score was determined through the following formula: Risk score = log [HLA-DQA2 * (-0.410855864) + CCL13 * (-0.645973012) + GBP1* (-0.081755076) + LAMP3* (-0.185669508) +SLC7A11*0.085404507]. The patients in the TCGA-TNBC training dataset were classified into two risk groups, and the OS probabilities of high-risk group were observably lower than those of low-risk group (Fig. 5B). Moreover, the patients exhibiting higher risk scores were more susceptible to death, and the AUC value was higher than 0.7 in forecasting OS (Fig. 5B). Similar results were obtained based on GSE103091 (Fig. 5C), confirming the stability of this signature.

3.8. Establishment of a nomogram

Through Cox regression analyses, pathologic N and risk score were recognized as independent prognostic factors (Fig. 6A). A nomogram was established by these factors, which could forecast the OS of patients with TNBC (Fig. 6B). To interpret the nomogram, the points for each variable were assigned. Subsequently, the total points for a patient were calculated by adding up the assigned

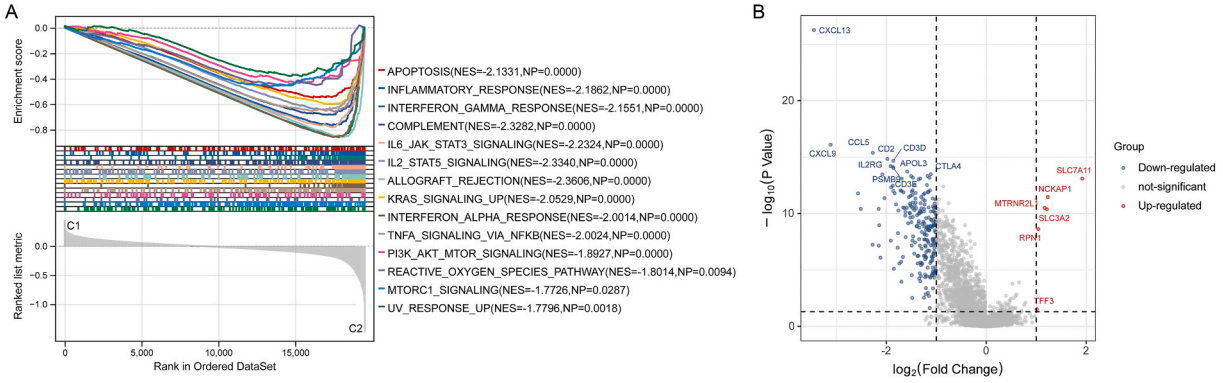

Fig. 4. Gene set enrichment analysis (GSEA) and identification of differentially expressed genes (DEGs) between two clusters. A: GSEA showed the differentially enriched hallmark gene sets between two clusters. B: Volcano plot of DEGs between two clusters. The blue and red dots represent downregulated and upregulated genes, respectively. (For interpretation of the references to colour in this figure legend, the reader is referred to the Web version of this article.)

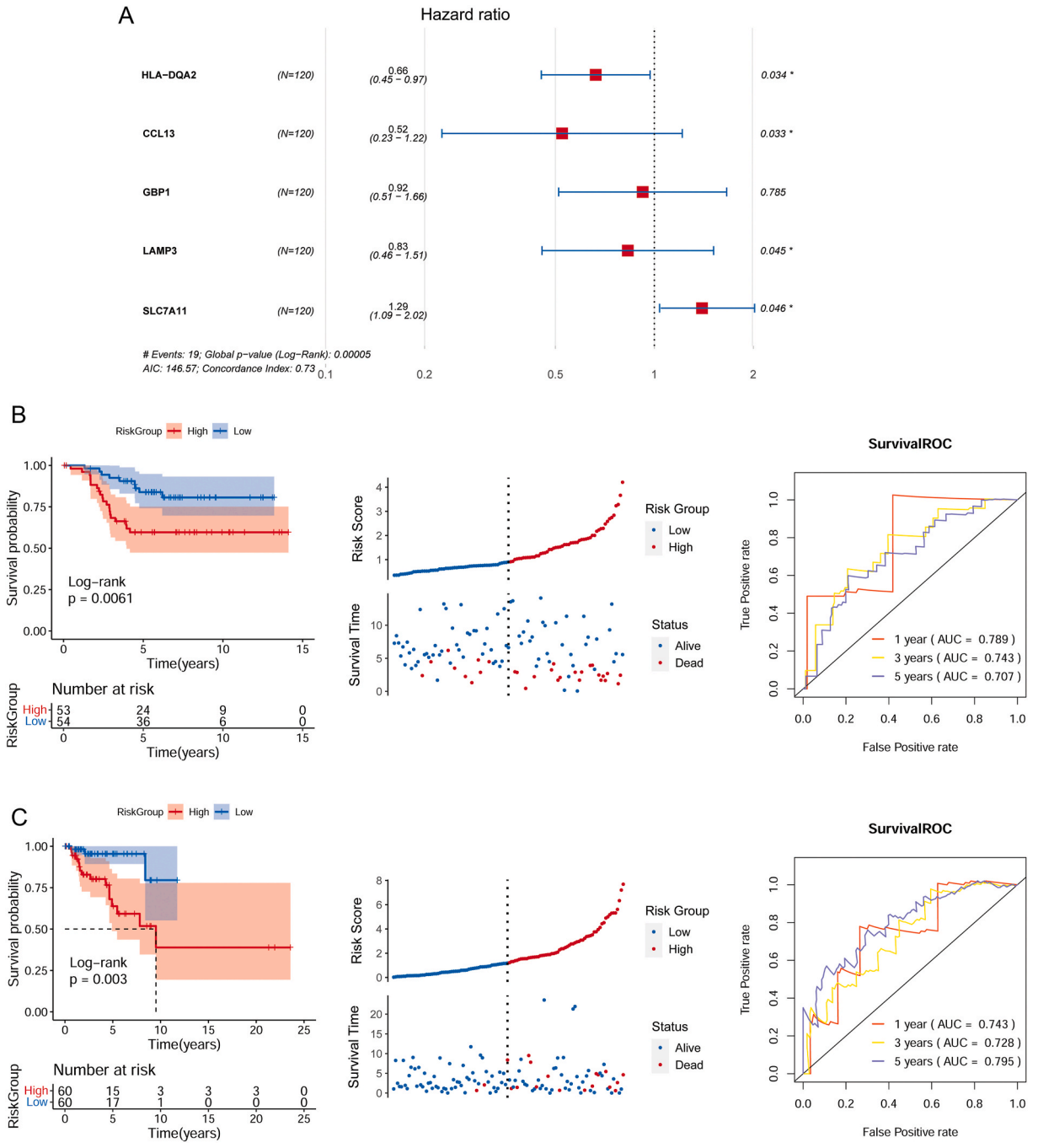

Fig. 5. Construction and validation of the prognostic signature. A: Stepwise Cox regression analysis revealed the optimal gene combination for construction of the prognostic signature. B: Analysis of the predictive performance of the prognostic signature based on TCGA-TNBC training dataset. C: Analysis of the predictive performance of the prognostic signature based on GSE103091 dataset.

points. By drawing a vertical line from the total points row, the probability of OS was determined. The calibration curves revealed a good alignment between the predictive and actual OS probabilities (Fig. 6C). Moreover, patients with high-nomogram score group demonstrated a poorer prognosis (Fig. 6D). Furthermore, the AUC value of nomogram was higher than 0.8 in predicting OS (Fig. 6E). These data confirmed the high predictive accuracy of this nomogram.

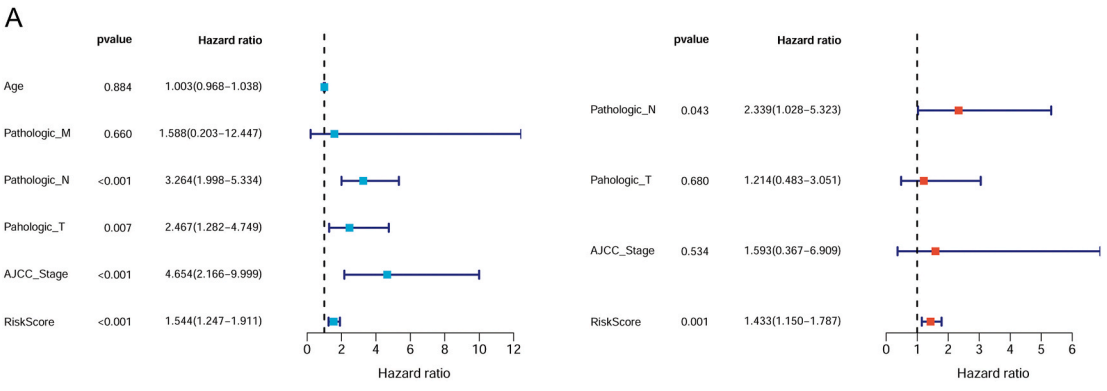

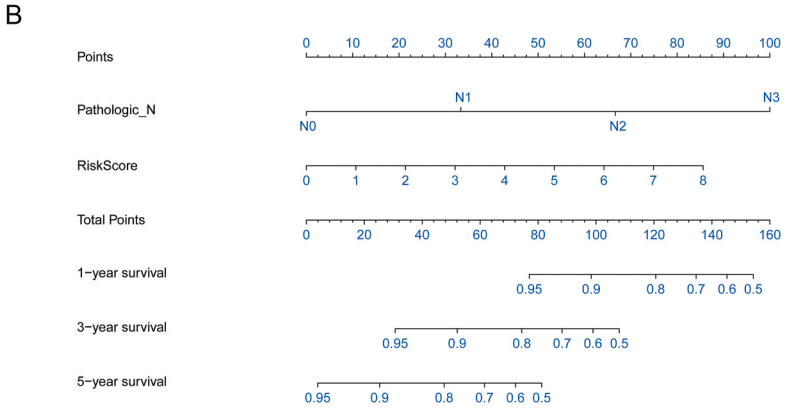

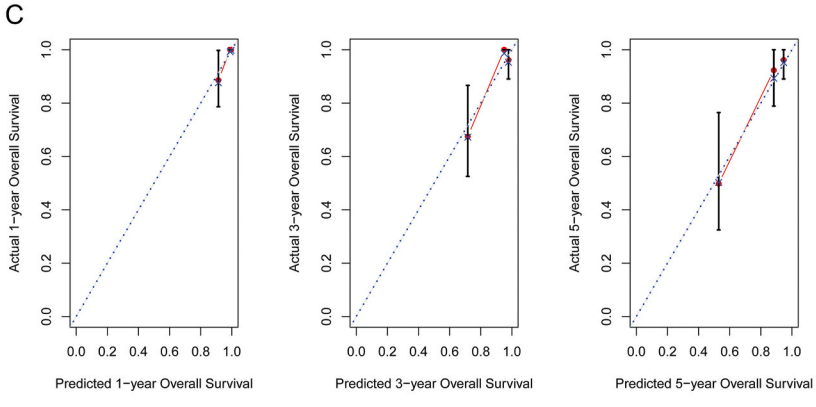

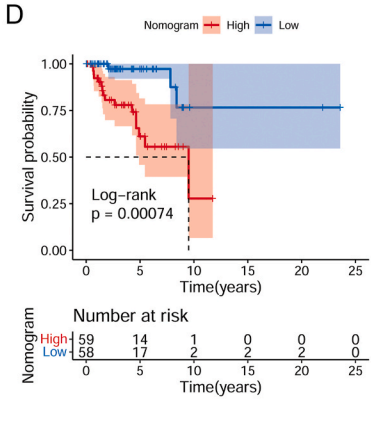

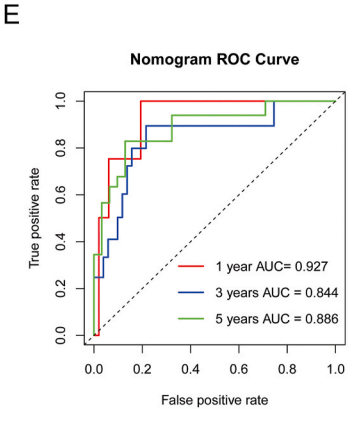

(caption on next page)

Fig. 6. Establishment and validation of a nomogram. A: Univariate and multivariate Cox regression analyses for screening independent prognostic factors. B: The constructed nomogram. C: The calibration curves of nomogram. D: The Kaplan-Meier survival curve showed the prognostic value of nomogram. E: receiver operating characteristic (ROC) curves showed the predictive performance of nomogram.

3.9. Drug sensitivity analysis for two risk groups

The sensitivity of 138 chemotherapy drugs in each patient was evaluated using the CDSC database. Three chemotherapy drugs that were most significant between the two risk groups were AMG.706, lapatinib, and imatinib, which had lower IC50 values in the high-risk group (Fig. 7A).

3.10. Association analysis of risk score with immunity

Immune infiltration analysis revealed substantial disparities in the infiltration proportion of 17 immune cell types between two risk groups (Fig. 7B). Moreover, the infiltration level of most immune cells was observably correlated with the prognostic signature genes (Fig. 7C).

3.11. Analysis of immunotherapy response of two risk groups

In terms of immunotherapy response, the TIDE scores were obviously higher in the high-risk group relative to the low-risk group. Moreover, the CYT and TLS scores were dramatically lower in the high-risk group (Fig. 7D). Additionally, the GSE103668 dataset was applied to validate the link between risk score and immunotherapy response. As expected, patients in the non-response group demonstrated markedly elevated risk scores relative to those in the response group (Fig. 7E).

3.12. Association analysis between clusters and different risk groups

The cluster distribution across different risk groups was examined. The data demonstrated a strong tendency for high-risk patients to be clustered into C1, whereas low-risk patients were primarily classified into C2 (Fig. 7F).

4. Discussion

TNBC represents a heterogeneous subtype of breast cancer with a poor prognosis. Exploring a reliable prognostic signature for TNBC may improve the clinical outcomes [29]. Disulfidptosis holds promise as a potential therapeutic target for cancer [13]. However, the role and regulatory mechanisms of disulfidptosis in TNBC remain unclear.

Here, we identified two disulfidptosis-related clusters, which had different OS and immune profiles. Moreover, we constructed a five-disulfidptosis-related gene signature (including HLA-DQA2, CCL13, GBP1, LAMP3, and SLC7A11), which was related to prognosis, immune infiltration, drug sensitivity, and immunotherapy response. Furthermore, we established a nomogram by pathologic N and risk score, which had a high accuracy for forecasting OS. Our identified disulfidptosis-related clusters and genes may have a great significance for the development of effective treatment strategy for TNBC.

TNBC is highly heterogeneous, resulting in different phenotypes and variable clinical outcomes. For cancer patients with multiple phenotypes and different prognosis, an individualized treatment strategy can achieve a better outcome [7], suggesting the clinical significance of tumor subtype identification. Molecular subtyping of TNBC through gene expression profiling is indispensable for deciphering the intricate molecular profiles of this heterogeneous disease and for crafting tailored treatment regimens [30]. A very recent study has also screened disulfidptosis-related subtypes of breast cancer on basis of the disulfidptosis-related gene expression, which can be used to stratify patients and guide treatment [31]. Similarly, this study identified two disulfidptosis-related clusters of TNBC, which provides valuable insights into the heterogeneity of TNBC and its prognostic implications. The finding that C1 showed a worse prognosis than C2 underscored the clinical relevance of these molecular subtypes in guiding patient management decisions. Also, C1 had more patients at III and IV stage than C2. These observations suggest that the molecular characteristics associated with disulfidptosis may play a crucial role in driving disease progression and influencing patient outcomes, and elucidating the molecular underpinnings of disulfidptosis could pave the way for developing targeted therapies and prognostic biomarkers to improve risk stratification and treatment strategies for TNBC.

Moreover, the infiltration proportion of key immune cells, like macrophages, exhibited significant difference between two clusters. A close link has been established between high infiltration of tumor-associated macrophages (TAMs) and increased risk of distant metastasis in patients with TNBC [32]. Zhang et al. also revealed that TAMs contributed to poor prognosis in TNBC [33]. Furthermore, most immune checkpoint genes and HLA family genes were highly expressed in C2. Immune checkpoint genes are pivotal in evading self-reactivity and stand as promising predictors for immunotherapy response [34]. HLA genes are important regulators in immune presentation and recognition. There is a substantial association between HLA gene expression and tumor immunologic features and patient prognosis [35]. These data indicate that patients in C2 may have a higher immunotherapy response than those in C1.

To further investigate the mechanisms mediating the different outcomes of disulfidptosis-related clusters, we identified DEGs between two clusters. Among these DEGs, five genes including HLA-DQA2, CCL13, GBP1, LAMP3, and SLC7A11 were selected for construction of a prognostic signature. HLA-DQA2 (Major Histocompatibility Complex, Class II, DQ Alpha 2) is one member of HLA

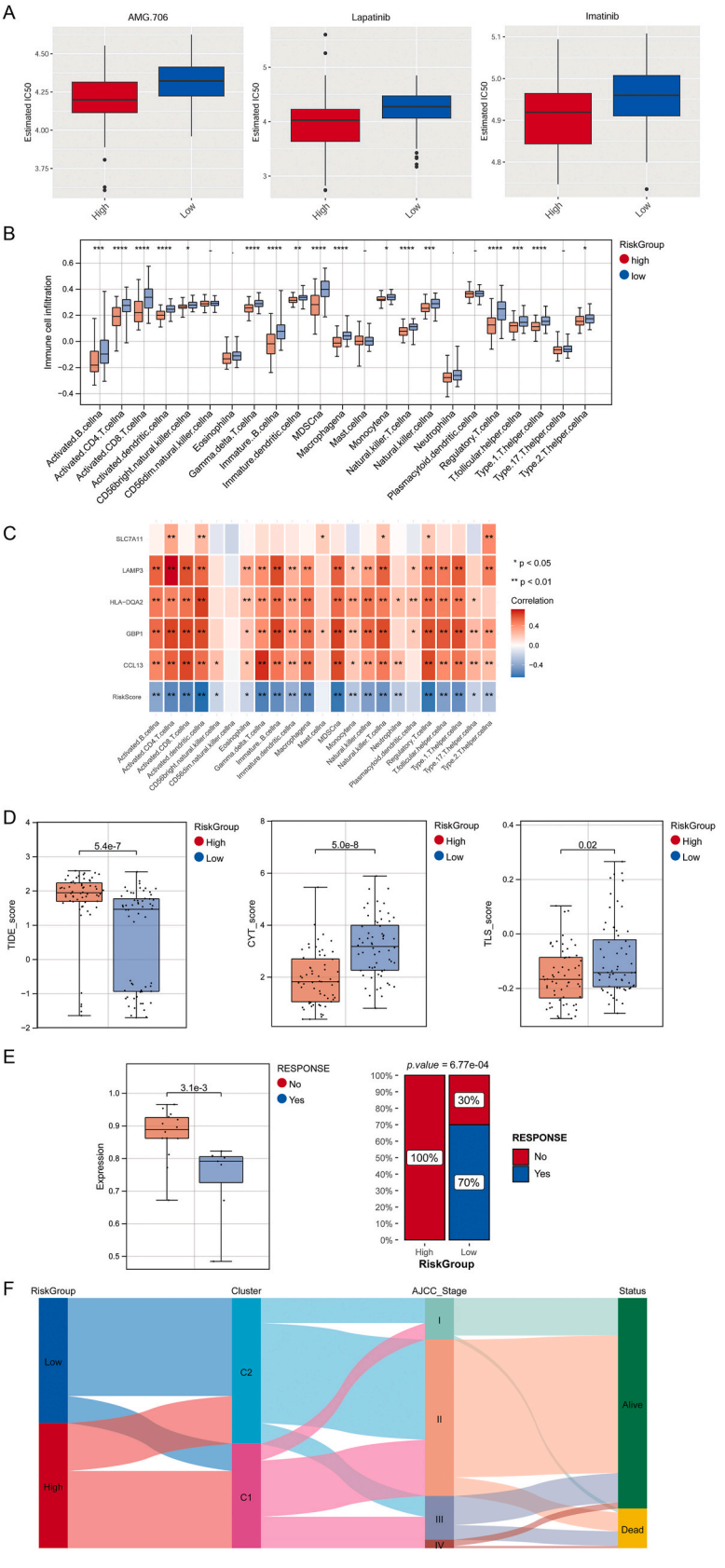

(caption on next page)

Fig. 7. Drug sensitivity, immune cell infiltration, immunotherapy response and cluster distribution of two risk groups. A: Drug sensitivity analysis showed the most significant drugs between two risk groups. B: The results of immune cell infiltration between two risk groups using the ssGSEA algorithm. C. The correlation between immune cell infiltration proportion and prognostic signature gene expression. D: Analysis of immunotherapy response of two risk groups, including TIDE, CYT and TLS scores. E: Analysis of the association between risk score and immunotherapy response using a validation dataset GSE103668. F: The association between cluster distribution and different risk groups. *P < 0.05, **P < 0.01, ***P < 0.001, and ****P < 0.0001.

class II genes that can affect the activity of MHC class II receptor [36]. A previous study has revealed the increased expression of HLA-DQA2 in breast cancer [37]. CCL13 (C–C Motif Chemokine Ligand 13) belongs to CC chemotactic factor family and is linked to the functionality of M2 macrophages [38]. Franzen et al. demonstrated that CCL13 could promote breast cancer cell proliferation [39]. GBP1 (Guanylate Binding Protein 1) belongs to the large GTPase family. GBP1 can be regulated by EGFR signaling in breast cancer cells and may be a therapeutic target for TNBC with elevated EGFR expression [40]. Moreover, LAMP3 (Lysosomal Associated Membrane Protein 3) exhibits elevated expression in TNBC tissues and is related to tumor metastasis [41,42]. SLC7A11 (Solute Carrier Family 7 Member 11) contributes to the development of various tumors via regulating cysteine transport. SLC7A1 is involved in breast cancer but there is little relationship between SLC7A11 and TNBC [43]. Notably, SLC7A11 is recognized as a major contributor of disulfidptosis [12]. In this study, a prognostic model was developed utilizing these genes, which had a good ability for predicting patients' OS. Therefore, we believe that our constructed disulfidptosis-related gene signature is valuable in predicting TNBC prognosis and the model genes may be novel prognostic biomarkers for TNBC. Moreover, a nomogram was established by pathologic N and our constructed prognostic model (risk score). Nomogram is confirmed as a visualization tool for predicting diseas prognosis and other clinical outcomes in cancer patients [44,45]. Our established nomogram demonstrated strong predictive capabilities for OS, potentially offering a straightforward and accurate approach for clinicians to assess the OS of TNBC patients.

Furthermore, we analyzed the chemotherapy drug sensitivity of different risk groups stratified by disulfidptosis-related gene signature, and high-risk patients showed a heightened sensitivity to chemotherapy drugs such as lapatinib. Lapatinib has shown to induce apoptosis in TNBC cells [46]. These data confirmed the clinical application of these chemotherapy drugs for patients with high-risk scores. Additionally, multiple immune cells had differential infiltration proportion between two risk groups, and high-risk patients exhibited increased TIDE scores and reduced immune response rates. These data suggest that low-risk patients may be more amenable to immunotherapy, offering a new insight for developing personalized treatment programs. Furthermore, we found that there is a strong tendency for high-risk patients to be clustered into C1, whereas low-risk patients were primarily classified into C2. These data indicate that patients in C1 might be more sensitive to chemotherapy drugs such as lapatinib, and patients in C2 are likely to be more suitable for immunotherapy. However, we did not analyze the drug sensitivity and immunotherapy response of two clusters, which need further investigation.

This research marks the inaugural effort to identify the TNBC subtypes linked to disulfidptosis and to establish a prognostic model on the basis of disulfidptosis-related genes. Moreover, this study analyzed the correlation of disulfidptosis-related subtypes and prognostic signature with the immune infiltration, clinical characteristics, and immunotherapy response of TNBC patients. Although disulfidptosis differs from other recognized cell death methods, our data obtained based on disulfidptosis-related genes not only facilitate to predicting TNBC prognosis, but also brings benefits to these patients with different risks by providing insights into their prognosis and enabling personalized treatment. Despite these, this study has several limitations. First, our analyses were all based on publicly available data, which may cause an inherent case selection bias. Second, the predictive value of the disulfidptosis-related prognostic signature was not validated using a clinical cohort. Our molecular subtypes and the model practicality and immunotherapy prediction accuracy in the TNBC population should be verified by more multicenter randomized controlled trials and immunotherapy datasets. Third, the expression of signature genes was not investigated using clinical TNBC tissues and their regulatory mechanisms in TNBC have not yet been experimentally explored. Collectively, further exploration through prospective studies and basic research is essential to perfect the details of this study.

In sum, two TNBC clusters linked to disulfidptosis were recognized, and C1 had a worse prognosis and a lower immunotherapy response than C2. Moreover, a five-disulfidptosis-related gene signature could be a powerful prognostic biomarker for TNBC, which was related to drug sensitivity of some chemotherapy such as lapatinib as well as immunotherapy response. Our findings lay a basis for accurate prognosis evaluation and personalized treatment for TNBC.

Data availability

The data underpinning the results of this study can be obtained from the corresponding author upon reasonable request.

Funding

National Natural Science Foundation of China with Project No. 11572200.

CRediT authorship contribution statement

Jie Wu: Writing – original draft, Conceptualization. **Yan Cai:** Visualization, Supervision, Data curation. **Gaiping Zhao:** Writing – review & editing, Methodology.

Declaration of competing interest

The authors declare that they have no known competing financial interests or personal relationships that could have appeared to influence the work reported in this paper.

Acknowledgement

Not applicable.

References

[1] M. Maqbool, F. Bekele, G. Fekadu, Treatment strategies against triple-negative breast cancer: an updated review, Breast Cancer (2022) 15–24.
[2] H. Katayama, P. Tsou, M. Kobayashi, M. Capello, H. Wang, F. Esteva, M.L. Disis, S. Hanash, A plasma protein derived TGFβ signature is a prognostic indicator in triple negative breast cancer, npj Precis. Oncol. 3 (2019) 10.
[3] M. Bou Zerdan, T. Ghorayeb, F. Saliba, S. Allam, M. Bou Zerdan, M. Yaghi, N. Bilani, R. Jaafar, Z. Nahleh, Triple negative breast cancer: Updates on classification and treatment in 2021, Cancers 14 (2022) 1253.
[4] R. Assidicky, U.M. Tokat, I.O. Tarman, O. Saatci, P.G. Ersan, U. Raza, H. Ogul, Y. Riazalhosseini, T. Can, O. Sahin, Targeting HIF1-alpha/miR-326/ITGA5 axis potentiates chemotherapy response in triple-negative breast cancer, Breast Cancer Res. Treat. 193 (2022) 331–348.
[5] G. Bianchini, J.M. Balko, I.A. Mayer, M.E. Sanders, L. Gianni, Triple-negative breast cancer: challenges and opportunities of a heterogeneous disease, Nat. Rev. Clin. Oncol. 13 (2016) 674–690.
[6] F.G. Dall'Olio, A. Rizzo, V. Mollica, M. Massucci, I. Maggio, F. Massari, Immortal time bias in the association between toxicity and response for immune checkpoint inhibitors: a meta-analysis, Immunotherapy 13 (2021) 257–270.
[7] V. Mollica, A. Rizzo, A. Marchetti, V. Tateo, E. Tassinari, M. Rosellini, R. Massafra, M. Santoni, F. Massari, The impact of ECOG performance status on efficacy of immunotherapy and immune-based combinations in cancer patients: the MOUSEION-06 study, Clin. Exp. Med. 23 (2023) 5039–5049.
[8] A. Rizzo, A. Cusmai, S. Acquafredda, L. Rinaldi, G. Palmiotti, Ladiratuzumab vedotin for metastatic triple negative cancer: preliminary results, key challenges, and clinical potential, Expet Opin. Invest. Drugs 31 (2022) 495–498.
[9] A. Rizzo, A.D. Ricci, L. Lanotte, L. Lombardi, A. Di Federico, G. Brandi, G. Gadaleta-Caldarola, Immune-based combinations for metastatic triple negative breast cancer in clinical trials: current knowledge and therapeutic prospects, Expet Opin. Invest. Drugs 31 (2022) 557–565.
[10] C. Chen, M. Shen, H. Liao, Q. Guo, H. Fu, J. Yu, Y. Duan, A paclitaxel and microRNA-124 coloaded stepped cleavable nanosystem against triple negative breast cancer, J. Nanobiotechnol. 19 (2021) 1–17.
[11] Y. Wang, Y. Jiang, D. Wei, P. Singh, Y. Yu, T. Lee, L. Zhang, H.K. Mandl, A.S. Piotrowski-Daspit, X. Chen, Nanoparticle-mediated convection-enhanced delivery of a DNA intercalator to gliomas circumvents temozolomide resistance, Nat. Biomed. Eng. 5 (2021) 1048–1058.
[12] X. Liu, L. Nie, Y. Zhang, Y. Yan, C. Wang, M. Colic, K. Olszewski, A. Horbath, X. Chen, G. Lei, Actin cytoskeleton vulnerability to disulfide stress mediates disulfidptosis, Nat. Cell Biol. 25 (2023) 404–414.
[13] P. Zheng, C. Zhou, Y. Ding, S. Duan, Disulfidptosis: a new target for metabolic cancer therapy, J. Exp. Clin. Cancer Res. 42 (2023) 103.
[14] S. Zhao, L. Wang, W. Ding, B. Ye, C. Cheng, J. Shao, J. Liu, H. Zhou, Crosstalk of disulfidptosis-related subtypes, establishment of a prognostic signature and immune infiltration characteristics in bladder cancer based on a machine learning survival framework, Front. Endocrinol. 14 (2023).
[15] A. Mayakonda, D.-C. Lin, Y. Assenov, C. Plass, H.P. Koeffler, Maftools: efficient and comprehensive analysis of somatic variants in cancer, Genome Res. 28 (2018) 1747–1756.
[16] T. Barrett, S.E. Wilhite, P. Ledoux, C. Evangelista, I.F. Kim, M. Tomashevsky, K.A. Marshall, K.H. Phillippy, P.M. Sherman, M. Holko, A. Yefanov, H. Lee, N. Zhang, C.L. Robertson, N. Serova, S. Davis, A. Soboleva, NCBI GEO: archive for functional genomics data sets–update, Nucleic Acids Res. 41 (2013) 27.
[17] M.D. Wilkerson, D.N. Hayes, ConsensusClusterPlus: a class discovery tool with confidence assessments and item tracking, Bioinformatics 26 (2010) 1572–1573.
[18] S. Hänzelmann, R. Castelo, J. Guinney, GSVA: gene set variation analysis for microarray and RNA-seq data, BMC Bioinf. 14 (2013) 1–15.
[19] A.A. Rizvi, E. Karaesmen, M. Morgan, L. Preus, J. Wang, M. Sovic, T. Hahn, L.E. Sucheston-Campbell, gwasurvivr: an R package for genome-wide survival analysis, Bioinformatics 35 (2019) 1968–1970.
[20] B. Chen, M.S. Khodadoust, C.L. Liu, A.M. Newman, A.A. Alizadeh, Profiling tumor infiltrating immune cells with CIBERSORT, Cancer Systems Biology: Methods and Protocols (2018) 243–259.
[21] B. Xiao, L. Liu, A. Li, C. Xiang, P. Wang, H. Li, T. Xiao, Identification and verification of immune-related gene prognostic signature based on ssGSEA for osteosarcoma, Front. Oncol. 10 (2020) 607622.
[22] D. Hu, M. Zhou, X. Zhu, Deciphering immune-associated genes to predict survival in clear cell renal cell cancer, BioMed Res. Int. 2019 (2019).
[23] J. Reimand, R. Isserlin, V. Voisin, M. Kucera, C. Tannus-Lopes, A. Rostamianfar, L. Wadi, M. Meyer, J. Wong, C. Xu, Pathway enrichment analysis and visualization of omics data using g: Profiler, GSEA, Cytoscape and EnrichmentMap, Nat. Protoc. 14 (2019) 482–517.
[24] G.K. Smyth, Limma: linear models for microarray data, Bioinformatics and computational biology solutions using R and Bioconductor (2005) 397–420.
[25] D. Zhu, S. Wu, Y. Li, Y. Zhang, J. Chen, J. Ma, L. Cao, Z. Lyu, T. Hou, Ferroptosis-related gene SLC1A5 is a novel prognostic biomarker and correlates with immune infiltrates in stomach adenocarcinoma, Cancer Cell Int. 22 (2022) 124.
[26] S. Zhang, Y.X. Tong, X.H. Zhang, Y.J. Zhang, X.S. Xu, A.T. Xiao, T.F. Chao, J.P. Gong, A novel and validated nomogram to predict overall survival for gastric neuroendocrine neoplasms, J. Cancer 10 (2019) 5944.
[27] P. Wen, J. Wen, X. Huang, F. Wang, Development and validation of nomograms predicting the 5-and 8-Year overall and cancer-Specific survival of bladder cancer patients based on SEER program, J. Clin. Med. 12 (2023) 1314.
[28] P. Geeleher, N. Cox, R.S. Huang, pRRophetic: an R package for prediction of clinical chemotherapeutic response from tumor gene expression levels, PLoS One 9 (2014) e107468.
[29] M.L. Disis, S.E. Stanton, Triple-negative breast cancer: immune modulation as the new treatment paradigm, American Society of Clinical Oncology Educational Book 35 (2015) e25–e30.
[30] S. Zhao, W.J. Zuo, Z.M. Shao, Y.Z. Jiang, Molecular subtypes and precision treatment of triple-negative breast cancer, Ann. Transl. Med. 8 (2020) 499.
[31] J. Liang, X. Wang, J. Yang, P. Sun, J. Sun, S. Cheng, J. Liu, Z. Ren, M. Ren, Identification of disulfidptosis-related subtypes, characterization of tumor microenvironment infiltration, and development of a prognosis model in breast cancer, Front. Immunol. 14 (2023) 1198826.
[32] Z.-Y. Yuan, R.-Z. Luo, R.-J. Peng, S.-S. Wang, C. Xue, High infiltration of tumor-associated macrophages in triple-negative breast cancer is associated with a higher risk of distant metastasis, OncoTargets Ther. (2014) 1475–1480.
[33] W.-j. Zhang, X.-h. Wang, S.-t. Gao, C. Chen, X.-y. Xu, Z.-h. Zhou, G.-z. Wu, Q. Yu, G. Xu, Y.-Z. Yao, Tumor-associated macrophages correlate with phenomenon of epithelial-mesenchymal transition and contribute to poor prognosis in triple-negative breast cancer patients, J. Surg. Res. 222 (2018) 93–101.
[34] F.F. Hu, C.J. Liu, L.L. Liu, Q. Zhang, A.Y. Guo, Expression profile of immune checkpoint genes and their roles in predicting immunotherapy response, Briefings Bioinf. 22 (2021).
[35] E. Schaafsma, C.M. Fugle, X. Wang, C. Cheng, Pan-cancer association of HLA gene expression with cancer prognosis and immunotherapy efficacy, Br. J. Cancer 125 (2021) 422–432.
[36] C. Lenormand, H. Bausinger, F. Gross, F. Signorino-Gelo, S. Koch, M. Peressin, D. Fricker, J.-P. Cazenave, T. Bieber, D. Hanau, HLA-DQA2 and HLA-DQB2 genes are specifically expressed in human Langerhans cells and encode a new HLA class II molecule, J. Immunol. 188 (2012) 3903–3911.

[37] G. Wu, G. Xiao, Y. Yan, C. Guo, N. Hu, S. Shen, Bioinformatics analysis of the clinical significance of HLA class II in breast cancer, Medicine 101 (2022) e31071.
[38] L. Li, F. Dai, L. Wang, Y. Sun, L. Mei, Y. Ran, F. Ye, CCL13 and human diseases, Front. Immunol. 14 (2023).
[39] B. Franzén, A. Alexeyenko, M. Kamali-Moghaddam, T. Hatschek, L. Kanter, T. Ramqvist, J. Kierkegaard, G. Masucci, G. Auer, U. Landegren, Protein profiling of fine-needle aspirates reveals subtype-associated immune signatures and involvement of chemokines in breast cancer, Mol. Oncol. 13 (2019) 376–391.
[40] M. Quintero, D. Adamoski, L.M.d. Reis, C.F.R. Ascenção, K.R.S.d. Oliveira, K.d.A. Goncalves, M.M. Dias, M.F. Carazzolle, S.M.G. Dias, Guanylate-binding protein-1 is a potential new therapeutic target for triple-negative breast cancer, BMC Cancer 17 (2017) 1–16.
[41] A. Nagelkerke, H. Mujcic, J. Bussink, B.G. Wouters, H.W. van Laarhoven, F.C. Sweep, P.N. Span, Hypoxic regulation and prognostic value of LAMP3 expression in breast cancer, Cancer 117 (2011) 3670–3681.
[42] Y. Zou, J. Xie, S. Zheng, W. Liu, Y. Tang, W. Tian, X. Deng, L. Wu, Y. Zhang, C.-W. Wong, Leveraging diverse cell-death patterns to predict the prognosis and drug sensitivity of triple-negative breast cancer patients after surgery, Int. J. Surg. 107 (2022) 106936.
[43] X. Tang, W. Chen, H. Liu, N. Liu, D. Chen, D. Tian, J. Wang, Research progress on SLC7A11 in the regulation of cystine/cysteine metabolism in tumors, Oncol. Lett. 23 (2022) 1–9.
[44] S. Liu, H. Xu, Y. Feng, U.D. Kahlert, R. Du, L.A. Torres-de la Roche, K. Xu, W. Shi, F. Meng, Oxidative stress genes define two subtypes of triple-negative breast cancer with prognostic and therapeutic implications, Front. Genet. 14 (2023) 1230911.
[45] W. Zhang, L. Ji, X. Wang, S. Zhu, J. Luo, Y. Zhang, Y. Tong, F. Feng, Y. Kang, Q. Bi, Nomogram predicts risk and prognostic factors for Bone metastasis of Pancreatic cancer: a population-based analysis, Front. Endocrinol. 12 (2021) 752176.
[46] C.-Y. Liu, M.-H. Hu, C.-J. Hsu, C.-T. Huang, D.-S. Wang, W.-C. Tsai, Y.-T. Chen, C.-H. Lee, P.-Y. Chu, C.-C. Hsu, Lapatinib inhibits CIP2A/PP2A/p-Akt signaling and induces apoptosis in triple negative breast cancer cells, Oncotarget 7 (2016) 9135–9149.